# Measuring saltation and creep with high spatial and temporal resolution

**Hans-Jürgen Schönfeldt**

**Summary**

Measurement of aeolian sand transport rates with high temporal and spatial resolution is crucial for further progress in developing proper sand transport equations, in testing and developing numerical models of sand movement by wind, and in the modelling of sand dunes, ripples and other aeolian forms. Observational research on the behaviour of sand grains in natural sediments under natural conditions is presented herein.

This study uses the established measuring principle of a Saltiphone (Spaan and Van den Abeele, 1991) and a webcam commonly used in personal computers. The webcam frame transfer is triggered every 0.1s by a sonic anemometer. Consecutive frames are compared and analysed in real-time by a computer program. The webcam signal also provides the number of moving grains also the grain size of the moving grains and this for every grain that has moved in a time step of 0.1s.

Problems to determine the transport near the thresholds and the difficulties in the determination of thresholds from measured mean transport rates are discussed, and proposals for dealing with the problems are made. An iterative technique to determine the thresholds of transport (ITT) from high resolution transport measurements is presented. In this way, constitutive equations for sand transport in terms of wind speed can be tested. If viable, they can be employed to infer estimates for the thresholds by minimising the root-mean-square error between measured and calculated transport data. Alternatively, the fluid and impact thresholds for aeolian sand transport are determined from the field measurements on a beach by analysing the onset and breakdown of saltation in gust and lull intervals (GLM) of rising and falling wind speeds, respectively.

**Zusammenfassung**

Für den weiteren Fortschritt bei der Entwicklung geeigneter Sandtransportgleichungen sowohl der Entwicklung und dem Test numerischer Modelle des durch den Wind verursachten Sandtransports und bei der Modellierung von Sanddünen, Sandrippeln und anderen äolischen Formen ist die Messung der äolischen Sandtransportrate mit hoher zeitlicher und räumlicher Auflösung Voraussetzung. Untersuchungen unter natürlichen Bedingungen über das Verhalten der Sandkörner im natürlichen Sediment werden vorgestellt.

Diese Studie beruht auf dem etablierten Messprinzip des Saltifons (Spaan and Van den Abeele, 1991) und benutzt eine handelsübliche Webcam, wie sie auch an einen PC angeschlossen werden kann. Der Webcam Frame Transfer wird durch ein Ultraschallanemometer jede 0.1s ausgelöst. Aufeinander folgende Bilder werden in Echtzeit durch ein Computerprogramm analysiert. Das Webcam Signal liefert sowohl die Anzahl der Körner als auch deren Größe, die sich im Abtastschritt von 0.1s bewegt haben.

Probleme der Transportberechnung nahe der Transportschwellen und Schwierigkeiten in der Bestimmung der Schwellen aus den gemessenen Transportraten werden diskutiert und es werden Vorschläge zum Umgang mit diesen Problemen gemacht. Es wird eine iterative Technik zur Bestimmung der Transportschwellen (ITT) aus hochaufge-

lösten Transportmessungen vorgestellt. Damit lassen sich Vorhersagegleichungen für den Sandtransport als Funktion der Windgeschwindigkeit testen. Wenn diese Vorhersagegleichungen sich als brauchbar erweisen, können diese zur Bestimmung der Schwellen durch Minimieren der mittleren quadratischen Abweichung zwischen gemessenen und berechneten Transport dienen. Alternativ werden die „fluid"- und „impact"- Schwellen des äolischen Sandtransports aus Feldmessungen an einem Strand durch Analyse des Einsetzens und des Abklingens der Saltation (GLM) in Windböen und Flauten bestimmt.

## Introduction

A number of equations have been proposed, which link horizontal sand fluxes with wind velocities (Bagnold 1941; Zingg 1953; Williams 1964; Kawamura 1964; Owen 1964; Gillette and Goodwin 1974; Gillette 1979; Lettau and Lettau 1978; White 1979; Sørensen 1985; Gillette and Stockton 1989; Leys and Raupach 1991; Shao et al. 1993; Stout and Zobeck 1997; Zheng et al. 2003, 2006; Stout 2004; Leenders et al. 2005). Bowker et al. (2007) compared the sand flux of model predictions with field measurements and then assessed the sensitivity of the simulations to several aspects such as the formulation of the sand flux equation and the specific value of the threshold velocity, $u_{*t}$. They used the transport equations of Kawamura (1964) and White (1979) (Eq. (1)) and of Owen (1964) (Eq. (2)), with $Q$ as the transport rate, $u_*$ as the friction velocity and $A$, $A_1$ as constants. Kawamura and White's equation has a correction term reciprocally proportional to the friction velocity, but the difference between the measured and simulated data are nevertheless significant.

$$Q = A_1 u_*^3 \left(1 - \frac{u_{*t}^2}{u_*^2}\right)\left(1 + \frac{u_{*t}}{u_*}\right) \quad \text{Kawamura (1964), White (1979)} \qquad (1)$$

$$Q = A\, u_*^3 \left(1 - \frac{u_{*t}^2}{u_*^2}\right) \quad \text{Owen (1964)} \qquad (2)$$

Eq. (1) and Eq. (2) underestimate the measurement during the storm-event 1 in 2003 (see Bowker et al., 2007), and on storm 5 in 2003 the equations overestimate the measurements up to 100%. Storm 1 in 2004 cannot be predicted with this method. in the problem with the equations is the prediction of threshold friction velocity. Direct measurements of threshold friction velocity with a Sensit instrument have not solved the problem (Bowker et al., 2007). Both Stout (1998), with an experimental approach and Schönfeldt (2003) with a theoretical approach found that the averaging time of wind speed measurement affects the observed time fraction equivalence threshold.
Our current understanding of this problem lies in the nonlinearity of the transport equations with regard to friction velocity and in the use of different time scales for determining the variables. A simple reassessment of the problem as Schönfeldt (2003) has done leads to the conclusion that a transport equation must include the turbulence intensity of the wind, $I$, that is the relation of standard deviation in the wind, $\sigma$, to the mean wind speed $\bar{u}$. Mean wind speed equalling the threshold does not lead to transport in Eq. (1) and (2). Eqs. (1) and (2) provide negative transports for $u_* < u_{*t}$ and must actually be multiplied by the Heaviside function $H(u_* - u_{*t})$, with $H(x) = 0$ for

$x < 0$ else $H(x) = 1$. Introducing this, as well as using a Gaussian distribution for the wind (Stout and Zobeck, 1997), One gets the following simple analytical expression for the expected value of the wind during saltation (if $\bar{u} = u_{*_t}$), where the function $\varepsilon\{x\}$ denotes the expectation value of $x$,

$$\varepsilon\{u\} = u_s = \frac{1}{\sigma\sqrt{2\pi}} \int_{u_{*_t}=\bar{u}}^{\infty} u \cdot \exp(-\frac{(u-\bar{u})^2}{2\sigma^2}) du = \frac{1}{2}\bar{u} + \frac{\sigma}{\sqrt{2\pi}} \ . \qquad (3)$$

From Eq. (3) it is concluded that there is a conflict in the models. The expected value of the wind responsible for transport is not the mean of the wind, and sand will be transported; however, Eqs. (1) and (2) provide no transport. Unfortunately Eq. (3) cannot be inserted mathematically into Eqs. (1) and (2). The situation is, of course, more complicated. An analytical discussion of the Bagnold (1941) transport equation in relation to wind variability was done by Sørensen (1997). Following Jacksen (1997), the instantaneous transport is more linear and quadratic in $u$, not cubic. It can be stated

$$Q = a \cdot \varepsilon\{(u - u_{*_t})\} + b \cdot \varepsilon\{(u - u_{*_t})^2\}. \qquad (4)$$

Eq. (4) is analytically resolvable. Analogous to Eq. (3), the expectation value of $Q$ (Eq. (4)) involves in addition to the mean wind speed terms of $\sigma$, $\sigma^2$ and mixed terms.
This analytical issue will not be pursued: the problem is yet more complex. According to Bagnold (1941), there are two thresholds for saltation: the fluid threshold, which is defined as the wind speed at which particles start moving due to the forces of wind only, and the impact threshold, which is the speed at which the combined action of wind forces and saltation impacts can only sustain movement. This means that grain movement by a fluid has a characteristic hysteresis and is strongly nonlinear. The saltation process depends on how frequently the wind speed exceeds the fluid threshold and then how long the wind speed stays over the impact threshold. The same mean wind speed may provide different transport rates, depending on statistical parameters of the wind. Schönfeldt (2008, 2011) has introduced these two thresholds in a transport equation of Sørensen (2004) for homogeneous sand of sizes greater than 125 µm, based on measurements of Iversen and Rasmussen (1999)

$$Q = \frac{\rho}{g} u_{*_t}^3 \left( \gamma V^2 + \beta V - \gamma - \beta \frac{1}{V} \right), \qquad (5)$$

where $V = u_* / u_{*_t}$ denotes the dimensionless friction velocity or, transformed to the short time scale, the dimensionless saltation scaled wind speed at arbitrary hight $z$ well above the saltation height ($V = u(z)/u_t(z)$), $\rho$ the density of the air, $g$ the acceleration of gravity and $\beta$ and $\gamma$ are graindiameter-dependent constants. In this transport equation derived from wind tunnel data, Schönfeldt (2008) replaced the powers of $V$ by its expected values during saltation, and the non-written Heaviside function in the transport equation by the probability of saltation $F$. The expected values are functions of $V$, relation of the mean wind speed to the impact threshold, turbulence intensity $I$ and $r_1$, and autocorrelation of the wind at lag one $\Delta t$.

$$Q = \frac{\rho}{g} u_{*t}^3 F(V, I, r_1)\left( \gamma\varepsilon\{V_s^2\} + \beta\varepsilon\{V_s\} - \gamma - \beta\varepsilon\left\{\frac{1}{V_s}\right\}\right) \qquad (6)$$

Near the thresholds, transport based on wind with a distribution function can deviate up to 100% from the transport calculated with the same constant mean wind speed. In Figure 1, transport $Q$ is shown as function of the mean scaled wind speed with the parameters $I$ and $r_1$, based on the Sørensen (2004, Eq. (5)) equation and a Gaussian distributed wind. Note that all these curves are based on the same scaled impact threshold $Vi$ = 1, and, according to Bagnold (1941),

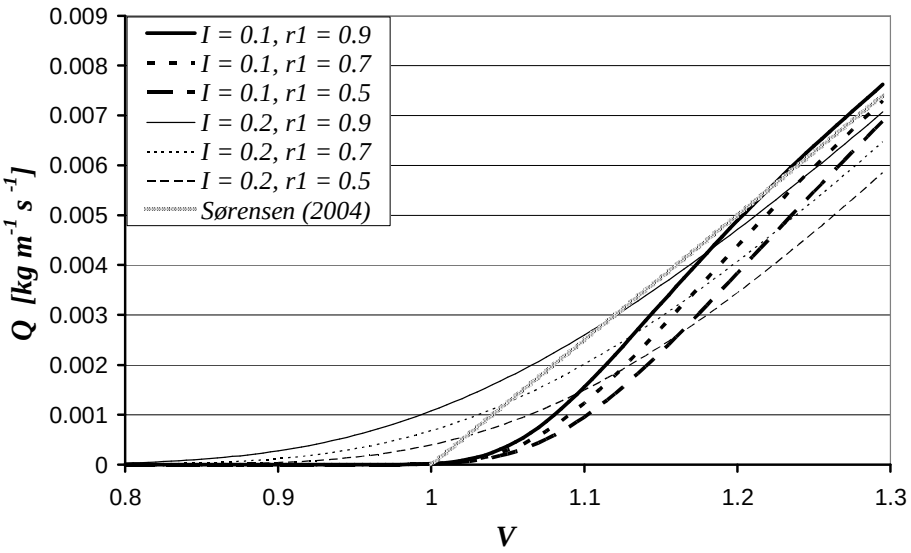


**Fig. 1:** *Sand transport Q as function of the scaled saltation velocity V with the turbulence intensity I and the autocorrelation $r_1$ as parameters (Schönfeldt, 2008, 2011).*

on the same scaled fluid threshold of $Vf$ = 1.25. It is apparent that a meaningful threshold is never obtained by extrapolation of the transport to zero. Methods such as the time fraction equivalence method (TFE, Stout and Zobeck, 1996) or the fractionating in count rate method (Schönfeldt, 2004) provide only one threshold. Using synthetic time series of transport with the two Bagnold (1941) thresholds, these methods differ and do not find the thresholds introduced in the synthetic time series depending on the statistical parameters of the wind. The distribution functions of the powers of wind speed during saltation are indeterminate without knowledge of the thresholds. The key variables are the thresholds. They depend not only on the grain diameter, but also on the humidity of the bed and must be determined experimentally by testing transport equations with field observations.

In the following, two methods of threshold determination are discussed, both of which both provide a fluid and an impact threshold. We will show the need of high resolution sensors for determination of the two thresholds. Furthermore we provide thresholds of a natural mixed sand bed in dependence of the grain diameter.

## Material and methods

1. The gust and lull method to determine the fluid and impact thresholds (GLM)

The gust and lull method (GLM) to determine the thresholds was introduced by Schönfeldt (2004) and is strictly based on the Bagnold's (1941) findings of the properties of the two thresholds. The basic idea is that in an intermittent transport there are periods with transport (gusts) and periods without transport (lulls). In the GLM, the time series of moving grains (data of Saltiphone, Sensit, Safire, etc.) were searched for periods with zeros following periods of saltation, and for periods of saltation following periods of zeros. Only periods with a minimum number of consecutive zeros followed by the same number of consecutive values greater than zero will be used from the data set for a gust interval, and vice versa for a lull interval. The fluid threshold is then calculated as the mean of wind speed on the sampling point preceding saltation and the wind speed on the sampling point on which saltation was first observed. The impact threshold is calculated as the mean of wind speed on the first sampling point without saltation and the wind speed on the preceding sampling point with saltation. In developing the method, Schönfeldt (2004) did not take into account that the time series of saltation lags behind the wind, but it is not a simple time shift of the two series. The time series of saltation is predicted by a transfer function of the wind time series. The transfer function can be established by exponential functions with a time constant (characteristic response time) $\tau$ without time shift (Pfeifer and Schönfeldt, 2012). Using these findings, GLM can be evaluated.
Figure 2 shows a sinusoidal, scaled wind-speed alteration with a relatively long period of 40 seconds. On the fluid threshold ($V$ = 1.25), the saltation starts. Two models of transport reaction are plotted: an immediately reaction of saltation on wind speed (thick dotted line), and an exponential transfer function described by Eq. (7) with $\tau$ equal to 0.7 seconds (thick dashed line).

$$Q(t) = \int_{0}^{-\infty} H(V(t-\xi)Exp(-(t-\xi)/\tau) \cdot V(t-\xi)d\xi \qquad (7)$$

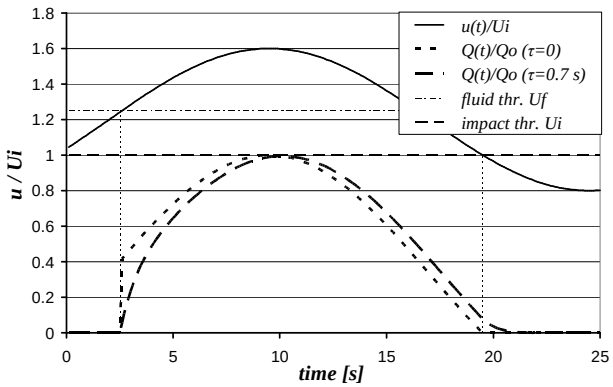


**Fig. 2:** *A scaled, sinusoidal wind-speed alteration with a period of 40 seconds and the reaction to the saltation activity with two models: an immediate reaction of saltation on wind speed (thick dotted line), and an exponential transfer function with τ equal to 0.7 seconds (thick dashed line; this curve has the 'saw-tooth' shape also recovered in the measurements of Butterfield (1999)).*

Eq. (7) is the convolution of wind speed with exponential transfer function of the wind to saltation activity in a linearized form. The sinusoidal gust produces a typically 'saw-tooth' shaped curve of transport also recovered in the measurements of Butterfield (1999). The transport has 8% of the steady state if the wind goes below the impact

threshold ($V$ = 1). The GLM underestimates the impact threshold by up to 16%, depending on the resolution of the sensor used. A response time of 1.6s, as predicted by Butterfield, enlarges the error. On the other hand, the GLM provides exactly the fluid threshold and never the impact threshold if the response of saltation to wind speed fluctuations is a decay curve. Similar to Schönfeldt (2004), the GLM was tested using arbitrary time series of wind speeds. The time series of wind speed was modeled as a first-order autoregressive Markov process and the saltation activity, in contrast to Schönfeldt (2004), with Eq. (7) to produce an exponential transfer.

## 2. The iterative technique to determine the thresholds of transport (ITT)

Given the deficiency of the GLM, a method was developed to take a transfer function of wind to saltation activity into account. This method is described by Schönfeldt (2012). The method uses arbitrary transfer weights. The ITT provides thresholds from measured time series of wind and saltation activity. For this purpose, a discrete formulation of Eq. (7) is helpful:

$$Q_{approach}(j) = \sum_{i=0}^{N} h(j-i)\, f_{h(t=0)}(i) \cdot (u(j-i) - u_i) \qquad (8)$$

Variables are defined as follows. *Variable* $u(j)$ is the measured wind speed at time $j$; scaled wind speed was not used, the impact threshold $u_i$ is unknown; $h(j)$ is the status of saltation and performs like the Heaviside function; $h(j)$ is equal to 1 if the wind speed is equal to or higher than the fluid threshold $u_f$ ( $u(j) \geq u_f$ ) and remains 1 if the wind speed stays above the impact threshold which involves $h(j\text{-}1) = 1$ (the previous time step was saltation and it will be sustained because $u(j)$ is greater than the impact threshold). In all other cases, $h(j)$ is equal to zero. Variables $f_1(i)$ are the transfer weights on the time shift $i\Delta t$ if $h(j=0) = 1$ (saltation begins or sustains), and $f_0(i)$ are the transfer weights on the time shift $i\Delta t$ if $h(j=0) = 0$ (saltation stops and dropout). $Q_{approach}(j)$ is a sand transport approach. The task of the ITT is to vary all these parameters on the right hand side of Eq. (8) such that

$$rmse = \sqrt{\frac{1}{M}\sum_{j=1}^{M}\left(\frac{Q(j)approach}{\sigma_{Q_{approach}}} - \frac{Q(j)_{measured}}{\sigma_{Q_{measured}}}\right)^2} \qquad (9)$$

will be a minimum. Essentially, two sets of transfer weights on $N$ +1 nodes, and the two thresholds are to vary. If we use $N$ = 30, we have 60 variables to vary, $f_1(0)$ can be set to 1 and $f_0(0)$ to zero ($h(j=0) = 0$ per definition). Alternatively, it is possible to use a sum of three exponential transfer characteristics, three to start saltation activity and three to cease saltation activity

$$f_{h(0),k}(i) = a_{h(t=0),k} \exp(-i\Delta t / \tau_{h(0),k}), \qquad (10)$$

with $h(0) = 0, 1$ and $k = 1, 2, 3$. Then the $f_{h(t=0)}$ in Eq. (8) will be

$$f_{h(t=0)}(i) = \sum_{k=1}^{3} f_{h(t=0),k}(i). \qquad (11)$$

This process reduces the degrees of freedom from 61 to 11.
*rmse* as calculated after Eq. (9) may have secondary minima. In this case, it is not easy to find the absolute maximum with a numerical program by varying the parameters. In the reviewed cases, start parameters could be varied and the minimum for *rmse* was always the same, but with somewhat other weights $f_h(i)$. Insofar as the formulation of Eq. (10) is more particular, the numerical noise from one transfer weight to the other will be smoothed by the reduction to an exponentially transfer. In order to get the same minima with Eq. (10), not less than two to three characteristic response times are required.

## 3. Study site

Field experiments were carried out on the beach of Zingst in the North East part of the peninsula Fischland-Darß-Zingst on the Baltic Sea (54°26' N, 12°42' E) during the spring of 2011. This beach is 18 km long, orientated along an East-West direction. Surface of the beach was covered with dry quartz sand with a mean grain diameter of 400 µm. To remedy beach erosion in the past, gravellike material was hydraulically pumped onto the beach. Consequently, the size distribution of moving grains and of those on the surface was variable, depending on the wind direction. Slightly onshore winds activate finer sand from the foreshore/berm, and longshore winds activate the gravel-like particles from the backshore/beach. The prevailing wind direction is in the form of longshore westerlies. Measurements were carried out under such longshore winds, in order that fetch differences do not influence the measurements. In Figure 3, the instrument array is depicted. The Guelph sand trap was used to compare the measured webcam grain- size distribution with the sieved contends of the trap. An array of six microphones (black diaphragms in Fig. 3) works as array of six Saltiphones. The miniaturisation of the microphones (Saltiphones) leads to a less intense intervention in the flow and permit a fine sensing near the ground (the nearest two are 0.015 m above the ground level). A sonic anemometer was buried into the sand so that the centre of the sampling volume was at a typical height of 0.1-0.2 meters. This low measuring height was used to minimise the effect of time shift in the wind field as reported by van Boxel et al. (2004). This measuring position of the sonic is acceptable especially near the thresholds, i.e. in periods of low saltation intensity.
The webcam is a relatively new measuring device in measuring aeolian sand transport and is described by Schönfeldt (2012). The webcam observe the sand (beach surface) from a distance of 8 cm and has a resolution of 640 x 480 pixels. One pixel equates 0.1 x 0.1 mm on the beach surface. The webcam frame transfer is triggered by the sonic every 0.1 s. A laptop computer (shadow of the laptop, mounted on a tripod appears on the left in Fig. 3 behind the sonic) records data sequentially from the sonic, the webcam data generated parallel to the sonic, and microphone data, all in one file. Thereby, it will prevent a time shift in between the signals of the different instruments.
The guiding principle in webcam signal generation is that a previous frame will be compared to a current frame pixel by pixel. Where differences occur, a grain has moved. The software detects it and records the place of change. The postprocessing program arranges the pixels and provides grain sizes. The maximum usable frame rate is limited by the maximum usable data transfer. This frame rate is too low, and the exposure time of the webcam is too long for observation of saltating grains. The web-

cam cannot see moving grains, i.e., the moving grain appears as a shadow in the picture and is smaller than the noise. Creeping grains also move fast, but yet every saltating and creeping grain causes a change in light reflection on the start position and/or on the arrival point. Simply, the webcam signal is proportional to the number of grains that, on average, leaves and arrives in the webcam's visual field of the beach surface (6.4 x 4.8 cm). The webcam has potential in characterization of grain-size distribution (examination of sieved grain fractions in a wind tunnel), and the application of microphones is described in Schönfeldt (2012).

**Fig. 3:** *The instrument array. From left to right: Guelph sand trap, web cam, microphone array of six microphones (work as Saltiphones), and sonic anemometer (buried).*

## *Results*

Figure 4*a* shows the grain-size distribution of the contents of the Guelph sand trap after one hour exposure, together with the distribution measured by the webcam and the surrounding surface grain-size distribution. The curves in Figure 4*a* are normalized such that the sum of distribution bins multiplied by the bin distance $\Delta D$ is equal to 1. The different resolution of sieve set and webcam leads to different height of maxima. Nevertheless, the webcam overestimates the grains of size less 0.2 mm.
The Guelph sand trap has measured a sand transport of 0.001 kg $m^{-1}$ $s^{-1}$ and the webcam on average has determined 160 moving grains in one time step of 0.1 s, but only in 38% of the measuring time of one hour did the webcam record saltation activity. The maximum recorded activity was 2405 grains in one time step of 0.1 s. The mean friction velocity was 0.19 m/s, the turbulence intensity 0.41, and the autocorrelation of the wind $r_1$ = 0.966. On that day, the wind was extremely turbulent, and the measurement was suitable for the two above stated methods GLM and ITT.

In Figure 4*b*, grain-size distribution as measured the webcam is compared with sieved samples from the Guelph trap. Strong winds have activated gravel-like material which was hydraulically pumped onto the beach to remedy beach erosion. The shift of the maximum of the grain-size distribution is seen in the sieved probes as well as in the webcam signal. The particle-size distribution determined by sieving of the content of a Guelph sand trap after 10 minutes exposure is very similar to that determined with the web cam during the same time period. More results are given by Schönfeldt (2012).
As documented in Figures 4*a* and *b*, the webcam can clearly resolve grain size, and consequently the webcam was used to determine the thresholds. The thresholds (Fig. 5) are measured on the beach of Zingst using the webcam and the microphones, not measurements in a wind tunnel using different grain-size fractions. The bed is a mix of grains of different sizes (Fig. 4*a*). The software determines the diameter, sorts the grains and determines the thresholds using the GLM and ITT method.

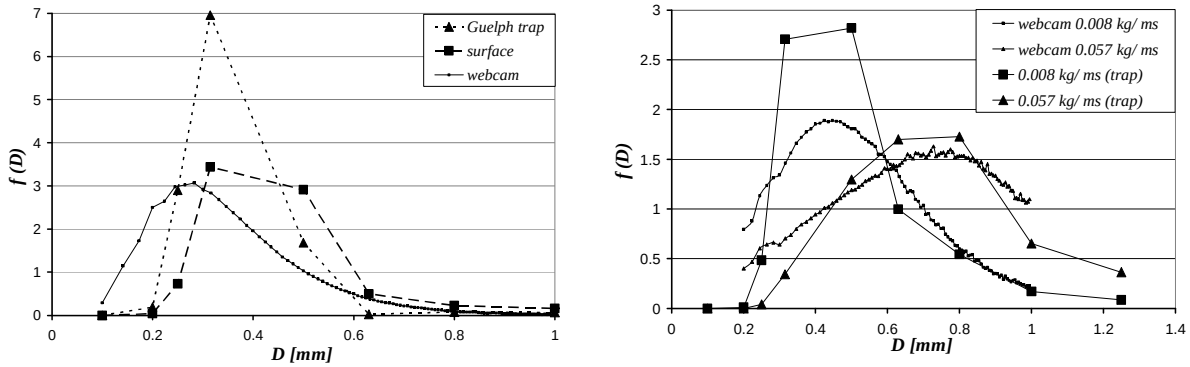


**Fig. 4*a*:** (left) *Grain-size distribution from 14.02.2011, dotted line - the contents of the Guelph sand trap, dashed line - the grain-size distribution of the uppermost 2 mm of the investigated area, and solid line - the grain-size distribution as measured the web-cam.*
**Fig. 4*b*** (right) *The mean grain-size distribution for ten minutes on24.03.2011, large symbols - the contents of the Guelph sand trap, small symbols - the grain-size distribution as measured with the webcam. The shift to the maximum grain size was caused by strong wind which activated the gravel-like material pumped onto the beach to remedy beach erosion.*

Given the errors of the GLM (see above), the two methods were tested with synthetic time series. A detailed variation of the parameters as Schönfeldt (2011) has used for the transport will be passed on. The parameters of the arbitrary time series of wind speed are adapted to the mean, the standard deviation and $r_1$ of measured wind parameters on 14.02.2011. Time series of wind speed were modeled as a first-order autoregressive Markov process. Saltation activity was then modeled with Eq. (7) to produce an exponential transfer with a response time of one second ($\tau = 1$). The thresholds were selected such that the modeled transport activity was the same as in the measurements, which means transport occurred on 38% of the time. This is the same way of looking at the problem as Stout and Zobeck (1996), i.e., by determining the time fraction equivalence threshold of transport. In contrast to the latter, two scaled Bagnold thresholds ($Vi = 1$, $Vf = 1.25$) were used and received the scaled mean wind speed $\overline{V} = 0.8$, which caused 38% of saltation time activity in the synthetic transport time series.

The point of interest is not only the reaction of the methods on a response time, but also the reaction on noise in the signals. The wind speed on the webcam and the microphones is not the same as measured by the sonic, especially in the high frequency range. Successive noise is added to the synthetic time series, additive to the

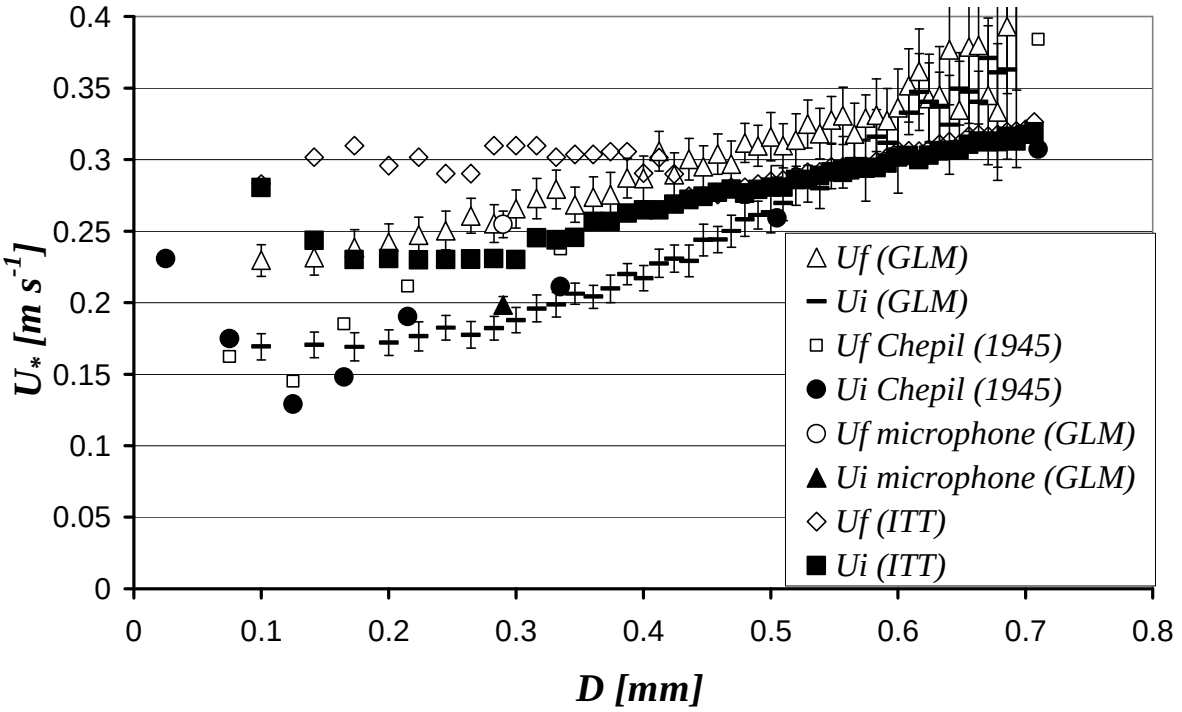


**Fig. 5:** *Fluid and impact thresholds occurring on 14.02.2011 determined using the gust and lull method (GLM; Schönfeldt, 2004), with the iterative technique to determine the thresholds of transport (ITT) described in the text and data from Chepil (1945). Error bars on the GLM thresholds denote the 90% confidence interval.*

wind and multiplicative to the transport. The rationale is that an additive noise to the transport in periods without saltation destroys the lull intervals and sometimes produces negative transport (the mean of the noise must be zero). The results are shown in Figure 6*a*. Note the axis of the abscissae is not absolutely correct, a result of the model used for noise. A random noise of 200% means that a Gaussian-distributed, non-correlated random noise with the same standard deviation as the model wind is added to the modelled wind speed and a non-correlated Gaussian random noise with the same standard deviation as the modelled saltation activity is multiplied with the saltation activity. The more or less variations from one point of calculation to the next are caused by the relatively "short" data length of 42345 observations, the same as existing data on 14.02.2011. Comparing the correlation coefficients of the noisy synthetic series (not shown in Fig. 6*a*) and the correlation coefficients of measured data (wind and approach saltation activity, $r \approx 0.9$), we can rate the noise in the measurements to 100 – 130%. The noisy synthetic time series of wind correlate with $Q_{approach}$ from one (no noise, *rmse* = 0.0005, Eq. (7)) to 0.37 (400% noise, *rmse* = 3.5). Without noise, the ITT method meets the thresholds exactly, the GLM underestimate the fluid threshold a bit and the impact threshold (*Vi* (GLM) = 0.71!) as given above. The departure from the value mentioned above is caused by the higher response time and the sensor used.

The program has no minimal threshold for saltation activity as a real sensor has. The program threshold is given by the number of transfer weights (N = 30); after three seconds, the transfer pipe (Eq. (8)) is broken off, and the saltation activity becomes zero in a lull interval.
The ITT method provides the transfer of wind to saltation activity as a by-product. In Figure 6*b* are transfer functions of wind to saltation activity shown. These are the transfer functions as a sum of the three exponential transfer characteristics (Eq. (11)), one if saltation and the second if the wind speed is lower than the impact threshold. The functions are standardised so that the integral over all of them is equal to 1. The two cases have three response times $\tau_{h,k}$, each with different corresponding amplitudes $a_{h,k}$ in Eq. (10).

### *Discussion*

The above sentence "the GLM provides exactly the fluid threshold and never the impact threshold if the response of saltation to wind speed fluctuations is a decay curve" must be modified. A correction factor must include, depending on the relation of mean wind speed to the thresholds and on $r_1$, the autocorrelation of the wind at lag one $\Delta t$. For the used statistical values and the thresholds, this factor is 1.016, less than 2 % of the value. If $r_1$ is lower as the used value of 0.966, the error becomes greater. The statistical error is caused by the calculation of the fluid threshold as the mean wind speed of the first sampling interval preceding saltation and the sampling interval in which saltation was first observed. These two values must be weighted by the probability of occurrence (see also Schönfeldt, 2004). With consideration of the statistical error, the GLM provides the fluid threshold.

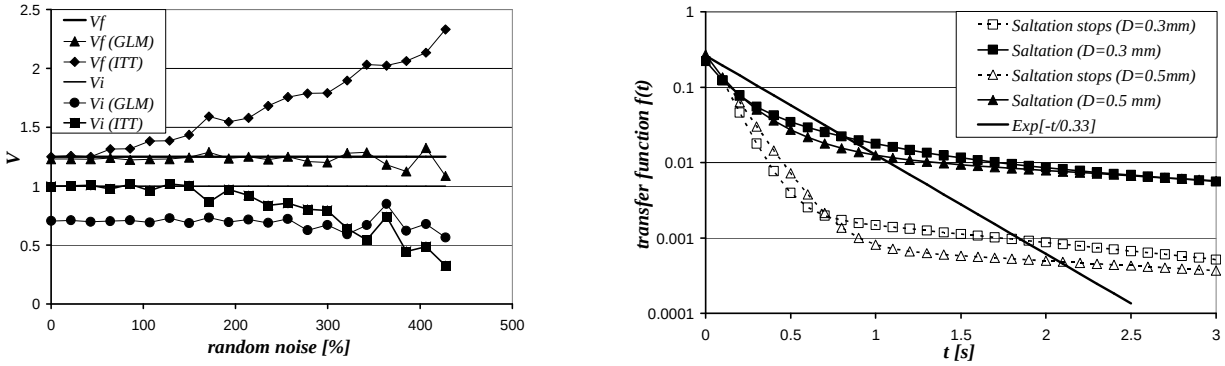


**Fig. 6*a*:** (left) *Thresholds determined by the GLM and ITT method as a function of additional noise. Vi and Vf are the default normalised impact and fluid thresholds, respectively.*
**Fig. 6*b*:** (right) *Transfer functions of wind to saltation activity for two grain diameters. The transfer during the gust intervals with saltation is denoted by "Saltation" and in a lull interval where the wind speed is lower then the impact threshold by "Saltation stops". For comparison, an exponential decay curve with τ = 0.33 s is plotted.*

The impact threshold determined by the GLM has also statistical errors and is additionally dependent upon the response time of saltation and the resolution of the used sensor. The GLM is not promising in determing the impact threshold. Conversely, the

ITT gives better impact thresholds as fluid thresholds when one considers additional noise. The ITT method seems to present reliable results for the impact threshold. In the region of the most recorded grains, the relation of $u_{*ITTimpact} / u_{*GLMfluid}$ is 0.89, the same as Chepil (1945) reported for this grain size. For a nearly uniform sand of average grain diameter 0.25 mm, Bagnold (1941, p. 57) obtained a fluid threshold friction velocity of 0.22 m $s^{-1}$ and an impact threshold friction velocity of 0.192 m $s^{-1}$, which results in a ratio of impact threshold to fluid threshold equal to 0.87. The absolute friction velocities measured here seems a little bit too high, but it must be kept in mind that the presented thresholds are measured on a bed with a mix of grains of different sizes, not on a bed with homogeneous sand.
Thresholds for grains smaller then 0.2 mm should be treated with caution; the webcam detects more grains than actually occur. These grains can be a mix of fine grains and "splintered" pixels from large grains. Grains greater than 0.6 mm are rather rare (see Fig. 4*a*). The confidence interval of the GLM shows that, too. Apart from this, the measured thresholds behave as the thresholds determined from the synthetic time series. On the other hand, it is not clear how the small grains influence the fluid threshold of large grains. If small grains are saltating, they can strike a larger grain and then the larger grain has sufficient energy to leave the bed. Given this issue, the measured thresholds are plausible.
The response of saltation activity on wind speed corresponds with the response time as determined by Pfeifer and Schönfeldt (2012) in cases of continuously saltating grains. In the case when saltation drops out, there are two equal response times. This means that two constants are sufficient to describe the drop-out process, but not so for beginning and maintenance of saltation. When the saltation begins and is sustained, there are three time constants necessary to describe saltation. In both cases, an exponential decay curve with $\tau$ = 0.33s drop out slow up more as the measured in the time scale of zero to two seconds, and then the measured transfer functions drop out slow up. The persistent stronger slow up of the transfer function in a lull interval is expected.

## *Conclusions*

Measurements show that the webcam is effective in measuring saltation with high spatial and temporal resolutions. The webcam provides useful results to determine the grain size distribution up to a tenth of a second. A gap yet persists in determining thresholds between the two methods, GLM and ITT. It is more a shortcoming of the methods than one of the webcam. The weak point of the ITT method is the high-frequency noise caused by the fact that wind and transport are not measured at the same place. The root-mean-square error between measured and calculated transport data has then a very flat absolute minimum.
Of the two methods for determining thresholds of saltation, acceptable errors were obtained for fluid threshold with the GLM and for impact threshold with the ITT. To reduce noise in the time series, distance between webcam and sonic could be reduced. A hot-wire anemometer in lieu of a sonic may be the way to entirely solve this problem. All in all, there is a wide application spectrum for a future use of the webcam or a similar camera system.

Acknowledgement
The article was improved thanks to comments from W. C. Johnson and Ch. Jacobi.

## References

Bagnold, R.A., 1941: The Physics of Blown Sand and Desert Dunes. Methuen, London, 256 pp.
Bowker, G.E., Gillette, D.A., Bergametti, G., Marticorena, B., Heist, D.K., 2007: Sand flux simulations at a small scale over a heterogeneous mesquite area of the northern Chihuahuan Desert. Journal of Applied Meteorology and Climatology 46(9), 1410-1422.
Butterfield G.R., 1999: Application of thermal anemometry and high-frequency measurement of mass flux to aeolian sediment transport research. Geomorphology **29**: 31–58.
Chepil, W.S., 1945: Dynamics of wind erosion. II. Initiation of soil movement. Soil Science **60**(4): 397-411.
Gillette, D.A., Goodwin, P.A., 1974: Microscale transport of sand-sized soil aggregates eroded by wind. J. Geophys. Res., 79, 4080–4084.
Gillette, D.A., 1979: Environmental factors affecting dust emission by wind erosion. Saharan Dust, SCOPE 14, C. Morales, Ed., John Wiley and Sons, 71–91.
Gillette, D.A., Stockton, H., 1989: The effect of nonerodible particles on wind erosion of erodible surfaces. J. Geophys. Res., 94, 12 885–12 893.
Iversen, J.D., Rasmussen, K. R., 1999: The effect of wind speed and bed slope on sand transport. Sedimentology 46, 723 – 731.
Kawamura, R., 1964: Study of sand movement by wind. Translated (1965) as University of California Hydraulics Engineering Laboratory Report HEL 2-8 Berkeley.
Jacksen, D.W.T., 1997: A new, instantaneous Aeolian sand trap design for field use. Sedimentology 43, 791-796.
Leenders, J.K., van Boxel, J.H., Sterk, G., 2005: Wind forces and related saltation transport. Geomorphology, 71, 357–372.
Lettau, K., Lettau, H., 1978: Experimental and micrometeorological field studies of dune migration. Exploring the World's Driest Climate, K. Lettau and H. Lettau, Eds., University of Wisconsin—Madison IES Rep. 101, 110–147.
Leys, J.F., Raupach, M. R., 1991: Soil flux measurements using a portable wind erosion tunnel. Aust. J. Soil Res., 29, 533–552.
Owen, R.P., 1964: Saltation of uniform grains in air. J. Fluid. Mech., 20, 225-242.
Pfeifer, S., Schönfeldt, H.-J., 2012: The response of saltation to wind speed fluctuations. Earth Surface Processes and Landforms, DOI: 10.1002/esp.3227.
Schönfeldt, H.-J., 2003: Remarks on the definition and estimation of the aeolian erosion threshold friction velocity. Meteorol. Z., 12, 137-142.
Schönfeldt, H.-J., 2004: Establishing the threshold for intermittent aeolian sediment transport. Meteorol. Z., 13, 3, 437-444.
Schönfeldt H-J. 2008: Turbulence and aeolian sand transport. (16.04.2008, EGU Vienna)
http://www.uni-leipzig.de/~meteo/en/orga/Schoenfeldt_EGU_2008_presentation.pdf
Schönfeldt, H.-J., 2011: Turbulence and aeolian sand transport. Wissensch. Mitt. aus dem Inst. f. Meteorologie d. Uni. Leipzig 48, 103-112.

http://www.uni-leipzig.de/~meteo/de/orga/LIM_Bd_48.pdf
Schönfeldt, H.-J., 2012: High resolution sensors in space and time for determination saltation and creep intensity. Earth Surface Processes and Landforms, DOI: 10.1002/esp.3228.
Shao, Y., Raupach, M. R., Findlater, P. A., 1993: Effect of saltation bombardment on the entrainment of dust by wind. J. Geophys. Res., 98, 12, 719–12 726.
Sørensen, M., 1985: Estimation of some Aeolian saltation transport parameters from transport rate profiles. Proc. Int. Workshop on the Physics of Blown Sand, Vol. 1, Aarhus, Denmark, University of Aarhus, 141–190.
Sørensen, M., 1997: On the effect of time variability of the wind on rates of Aeolian sand transport. Aarhus Geoscience, **7**, 73-77, (Department of Earth Sciences, University of Aarhus).
Sørensen, M., 2004: On the rate of aeolian sand transport. Geomorphology, 59, 53-62.
Spaan W.P, Van den Abeele G.D. 1991. Wind borne particle measurements with acoustic sensors. Soil Technology **4**: 51-63.
Stout, J.E., Zobeck, T.M., 1996. Establishing the threshold condition for soil movement in wind-eroding fields. Proceedings of International Conference on Air Pollution from Agricultural Operations, February 1996, Kansas City, Missouri, USA, Midwest Plan Service (MWPS C-3). Iowa State University, Ames, Iowa, USA, pp. 65–71.
Stout, J.E, Zobeck, T. M., 1997: Intermittent saltation. Sedimentology, 44, 959–970.
Stout, J.E., 1998: Effect of averaging time on the apparent threshold for aeolian transport. Journal of Arid Environments, 39, 395-401.
Stout, J. E., 2004: A method for establishing the critical threshold for aeolian transport in the field. Earth Surface Processes Landforms, 29, 1195–1207.
Van Boxel JH, Sterk G, Arens SM. 2004: Sonic anemometers in aeolian sediment transport research. Geomorphology **59**: 131–147.
White, B., 1979: Soil transport by winds on Mars. - J. Geophys. Res., 84, 4643-4651
Williams, G., 1964: Some aspects of the eolian saltation load. Sedimentology, 3, 257–287.
Zheng, X. J., Huang, N., Zhou, Y.-H., 2003: Laboratory measurement of electrification of wind-blown sands and simulation of its effect on sand saltation movement. J. Geophys. Res., 108, 4322, doi:10.1029/2002JD002572.
Zheng, X. J., Huang , N., Zhou, Y., 2006: The effect of electrostatic force on the evolution of sand saltation cloud. Eur. Phys. J. E, 19, 129–138.
Zingg, A. W., 1953: Wind tunnel studies of the movement of sedimentary material. Proc. Fifth Hydraulics Conf., Bulletin 34, Iowa City, IA, Institute of Hydraulics, 111–135.

**Address of the Author**

Hans-Jürgen Schönfeldt
University of Leipzig, Institute for Meteorology, Stephanstr. 3, D04103 Leipzig
e-mail: schoenfeldt@uni-leipzig.de